Available online at www.sciencedirect.com
ScienceDirect
Journal of Structural Biology 155 (2006) 395–408
Journal of Structural Biology
www.elsevier.com/locate/yjsbi

The discriminative bilateral filter: An enhanced denoising filter for electron microscopy data

Radosav S. Pantelic [a], Rosalba Rothnagel [a], Chang-Yi Huang [b], David Muller [b], David Woolford [a], Michael J. Landsberg [a], Alasdair McDowall [a,c], Bernard Pailthorpe [d], Paul R. Young [b], Jasmine Banks [e], Ben Hankamer [a,*], Geoffery Ericksson [f]

[a] *Institute for Molecular Bioscience, University of Queensland, Brisbane, Qld 4072, Australia*
[b] *School of Molecular and Microbial Sciences, University of Queensland, Brisbane, Qld 4072, Australia*
[c] *Centre for Microscopy and Microanalysis, University of Queensland, Brisbane, Qld 4072, Australia*
[d] *School of Physical Sciences, University of Queensland, Brisbane, Qld 4072, Australia*
[e] *Advanced Computational Modelling Centre, University of Queensland, Brisbane, Qld 4072, Australia*
[f] *Queensland Brain Institute, University of Queensland, Brisbane, Qld 4072, Australia*

Received 12 October 2005; received in revised form 23 March 2006; accepted 30 March 2006
Available online 19 May 2006

Abstract

Advances in three-dimensional (3D) electron microscopy (EM) and image processing are providing considerable improvements in the resolution of subcellular volumes, macromolecular assemblies and individual proteins. However, the recovery of high-frequency information from biological samples is hindered by specimen sensitivity to beam damage. Low dose electron cryo-microscopy conditions afford reduced beam damage but typically yield images with reduced contrast and low signal-to-noise ratios (SNRs). Here, we describe the properties of a new discriminative bilateral (DBL) filter that is based upon the bilateral filter implementation of Jiang et al. (Jiang, W., Baker, M.L., Wu, Q., Bajaj, C., Chiu, W., 2003. Applications of a bilateral denoising filter in biological electron microscopy. J. Struc. Biol. 128, 82–97.). In contrast to the latter, the DBL filter can distinguish between object edges and high-frequency noise pixels through the use of an additional photometric exclusion function. As a result, high frequency noise pixels are smoothed, yet object edge detail is preserved. In the present study, we show that the DBL filter effectively reduces noise in low SNR single particle data as well as cellular tomograms of stained plastic sections. The properties of the DBL filter are discussed in terms of its usefulness for single particle analysis and for pre-processing cellular tomograms ahead of image segmentation.

Keywords: Electron microscopy; Electron cryo-microscopy; Cryo-electron microscopy; Single particle analysis; Tomography; Image; Impulse noise reduction; Denoising; Filter; Bilateral; Anisotropic

1. Introduction

Advances in electron cryo-microscopy (cryo-EM) and image processing are resulting in the capture and recovery of structural information at rapidly increasing levels of resolution. Specifically, EM[1] tomography, single particle analysis, and electron crystallography are resolving the structures of subcellular volumes, macromolecular assemblies, and individual proteins, to ~50 Å (Baumeister, 2002), ~6 Å (Ludtke et al., 2004), and ~1.8 Å (Gonen

* Corresponding author. Fax: +61 7 334 62101.
E-mail address: b.hankamer@imb.uq.edu.au (B. Hankamer).

[1] *Abbreviations used:* 3D, three-dimensions/-dimensional; EM, electron microscope/microscopy; CTF, contrast transfer function correction; DBL filter, discriminative bilateral filter; FEG, field emission gun; GroEL, GroE chaperonin; KLH, keyhole limpet haemocyanin; FPLC, fast protein liquid chromatography; SNR, signal-to-noise ratio; TEM, transmission electron microscopy; CCD, charge coupled device; MSE, mean square error.

1047-8477/$ - see front matter
doi:10.1016/j.jsb.2006.03.030

et al., 2005), respectively. Furthermore, with the implementation of a new generation of electron microscopes fitted with 300 keV field emission guns (FEGs) and integrated aberration correction technology, current resolutions of ~0.7 Å (Zeneka and Van Mastrigt, 2005) have been achieved. Given further improvements in biological data collection methods (e.g. optimization of liquid helium (He) cooled stages, phase plates and increased data set sizes), considerable advances in structural resolution can be expected in the future.

Due to the sensitivity of biological samples to damage induced by high levels of electron exposure, images are typically collected at low doses (~10–30 $e^-/Å^2$) using a liquid nitrogen (N_2) (~77 K) or liquid He (~6–20 K) cooled stage to aid energy dissipation (van Heel et al., 2000). However the combined effect of imaging low contrast objects (such as individual macromolecular protein assemblies in vitreous ice) under low dose conditions is the capture of noisy, low contrast data. Relatively high noise levels across a whole range of frequencies occur due to the difference in ice thickness in which the sample is embedded, beam damage to the sample, incoherence in the electron beam (van Heel et al., 2000), shot noise (Downing and Hendrickson, 1999), cosmic rays, X-rays (Brink and Chiu, 1994; Downing and Hendrickson, 1999), and the point spread function of the detector (Downing and Hendrickson, 1999). Reported examples of high-frequency noise include hard X-ray events, which produce a signal near saturation over 1–3 pixels, and soft X-rays, which generate a signal corresponding to tens of electrons usually in one or two adjacent pixels (Downing and Hendrickson, 1999). The combined contribution of noise across the full frequency range of the image is clearly seen in the CTF graphs in which the noise level is represented by the plot connecting the minima (e.g., Sander et al. (2005)).

Central to the ability to resolve a 3D structure from such noise contaminated images is the ability to resolve the signal component. To date, electron crystallography has attained the highest resolution 3D reconstructions from any transmission electron microscopy (TEM) images (Mitsuoka et al., 1999). This is largely due to the periodic properties of 2D crystals, which allow the effective separation of signal (as diffraction spots) from noise by use of Fourier space techniques. In contrast, aperiodic objects, such as single particles, require alternative image denoising methods to facilitate the accurate detection, alignment and subsequent 3D reconstruction of individual molecular projections (van Heel et al., 2000). In the case of tomographic data sets, the presence of noise not only masks high-resolution detail, but also hampers automated image segmentation, which has the potential to accelerate the annotation of discrete subcellular volumes (Bartesaghi et al., 2005; Roerdink and Meijster, 2000; Volkmann, 2002).

Recently, Jiang et al. (2003) developed a bilateral filter (Fig. 1), based on the earlier work of Tomasi and Manduchi (1998). The most important property of this filter is its ability to reduce noise while preserving edge detail. In this respect Jiang et al. suggest that the bilateral filter is similar to anisotropic diffusion filters, and distinct from Gaussian filters (Fig. 1A) which smooth both noise and edge detail. The bilateral filter was shown to effectively denoise 3D reconstructions as well as electron cryo-micrographs of large particles such as rice dwarf virus (~50 nm diameter) and, to a more limited extent intermediate sized molecular assemblies such as the GroE chaperonin, GroEL (~850 kDa). However, large macromolecular assemblies yield higher SNR images than small molecules imaged under similar conditions, and such low SNR conditions limit the utility of the bilateral filter. This is because the bilateral filter identifies high amplitude/high frequency

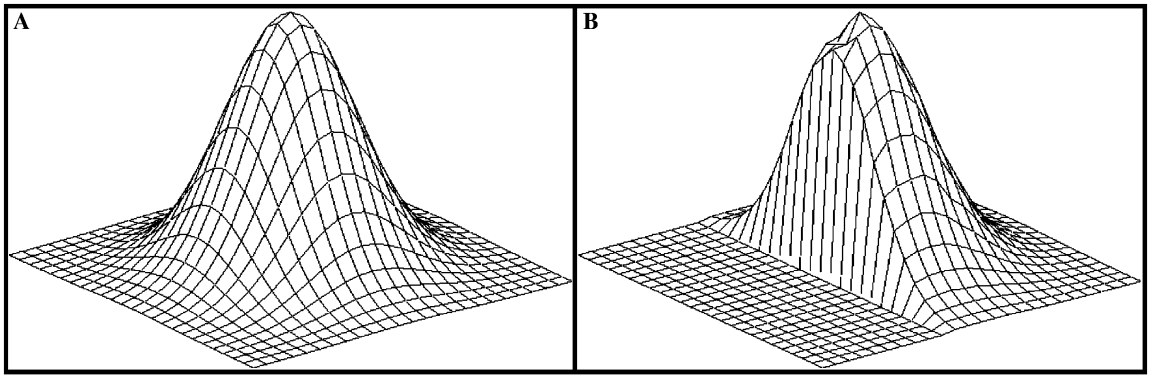

Fig. 1. The Gaussian and bilateral filters. (A) Gaussian filter. The 'chicken-wire mesh' describes the shape of the Gaussian filter. The central pixel located under the peak of the Gaussian filter is defined as the focal pixel (coordinates x,y). During the filtering process, a new intensity is calculated for the focal pixel based on the weighted intensities of surrounding pixels under the mask (coordinates m,n). The radius of the mask adjusts both the width of the mask, and the spatial weighting of the surrounding pixels (m,n). In a plateau region, the bilateral filter functions as a normal Gaussian filter. (B) Bilateral filter. The 'chicken-wire mesh' describes the shape of the bilateral filter. The central pixel located under the peak of the Gaussian filter is defined as the focal pixel (coordinates x,y). In a local region containing an edge, the bilateral filter calculates the new focal pixel's intensity based upon the weighted intensities of surrounding pixels under the mask (coordinates m,n) and on the same side of the edge. In this illustration the focal pixel is to the right of the edge. Pixels to the left are excluded from the filtering process. The bilateral filter therefore preserves edge detail. The bilateral filter has the limitation that it can also interpret impulse noise spikes as forming an edge.